渦電流探傷法による配管減肉評価のシミュレーション

Simulation for the Assessment of Wall Thinning using Eddy Current Method

(財)発電設備技術検査協会　程　衛英　Weiying CHENG　Member
(財)発電設備技術検査協会　古村　一朗　Ichiro KOMURA　Member

A pipe with protective lagging and thermal insulation is modeled by a multi-layered structure. Sinusoidal or pulsed eddy current are induced by a circular coil held above the structure to measure the thickness of the pipe wall. Analytical solutions of both sinusoidal and pulsed eddy current measurements are deduced. Parameters affecting the measurement are studied using the analytical solutions. Measurement conditions are discussed based on the analytical results.

Keywords: wall thinning, muti-layered structure, eddy current, pulsed eddy current, analytical solution

1. INTRODUCTION

The failure in pipelines in power plants, chemical plants, and other related industry systems accounts for huge economic loss . In order to ensure the integration of the piping system, pipe-wall thinning needs to be monitored appropriately. As illustrated in Fig. 1, the pipes are usually made of carbon steel which is thermal insulated and protected by aluminum, stainless steel, or galvanized steel cladding. The possible inspection methods are ultrasonic or radiographic testing. However, the conventional ultrasonic inspection requires the removal and reinstallation of insulation and cladding, good coupling between the sensor and the pipe, etc., which accounts for huge expense. Guide-wave ultrasonic inspection is fast but is regarded of suit for screening of corrosion area rather than exact assessment of the thinning rate and location. Radiograph inspection is slow and careful safety precaution is required. All in all, it remains a challenge for NDE to assess pipe-wall thinning efficiently and precisely.

Eddy current testing is well recognized for its rapid inspection speed. On the other hand, no contact with the test piece is required. This meets the request of no removal of insulation and cladding for pipe-wall thinning measurement. However, owing to the presence of insulation and electrically conductive cladding, eddy current induced in pipe is relatively weak, which makes the eddy current measurement of pipe-wall thinning a challenge comparing with conventional eddy current inspection. This study investigates the capability of eddy current method regarding pipe-wall thickness measurement via numerical simulation. In the primary stage, the piping system is modeled as a multi-layered structure. Analytical solutions of magnetic flux density of both sinusoidal and pulsed eddy current measurements are deduced. Parameters of the pipe structure and the measurement condition are studied via simulation.

連絡先: 程 衛英, 〒230-0044 (財) 発電設備技術検査協会, NDE センター, 電話 : 045-511-1376
E-mail: cheng-weiying@.japeic.or.jp

2. MODELING AND ANALYTICAL SOLUTIONS

2.1 Analytical Solution

If the diameter of a pipe is large enough, the pipe with insulation and cladding can be approximated by a four-layered structure illustrated in Fig. 2. From the top to bottom they are respectively the protective cladding, the thermal insulation, the pipe-wall, and the air inside. Their electrical conductivity and magnetic permeability

are respectively denoted by σ_i and μ_i (i=1,4).

A circular coil is positioned z_1 above the cladding, the inner and outer radius of the excitation coil are respectively r_1 and r_2, and the thickness of the coil is $z_2 - z_1$.

The general solution of vector potential A in each area of the multi-layered structure in Fig. 2 is given by the following equations [1,2],

$$A_I(r,z) = \int_0^\infty K(C_I e^{-\lambda_0 z} + B_0 e^{-\lambda_0 z})d\lambda_0$$

$$A_{II}(r,z) = \int_0^\infty K(C_{II} e^{\lambda_0 z} + B_0 e^{-\lambda_0 z})d\lambda_0$$

$$A_t(r,z) = \int_0^\infty K(C_t e^{\lambda_t z} + B_t e^{-\lambda_t z})d\lambda_0 \qquad (t=1,k-1)$$

$$A_k(r,z) = \int_0^\infty K(C_k e^{\lambda_k z})d\lambda_0 \qquad (1)$$

where k=4, I and II indicate the area above and below the excitation coil, C and B are coefficients to be decided. K is a parameter decided by excitation coil,

$$K = \frac{\mu_0 J_c}{2} J_1(\lambda_0 r) \frac{\chi(\lambda_0 r_1, \lambda_0 r_2)}{\lambda_0^3}, \qquad (2)$$

where $\chi(\lambda_0 r_1, \lambda_0 r_2) = \int_{\lambda_0 r_1}^{\lambda_0 r_2} x J_1(x)dx$, and $J_1(x)$ is the first type Bessel function, λ_0 is a parameter for integration.

By applying the boundary conditions between different layers, and the Cheng's matrix method [2], we have,

$$\begin{bmatrix} C_1 \\ B_1 \end{bmatrix} = T \begin{bmatrix} C_k \\ 0 \end{bmatrix} \qquad (3)$$

where $T = T(1,2) \times T(2,3) \times \cdots \times T(k-1,k)$, and

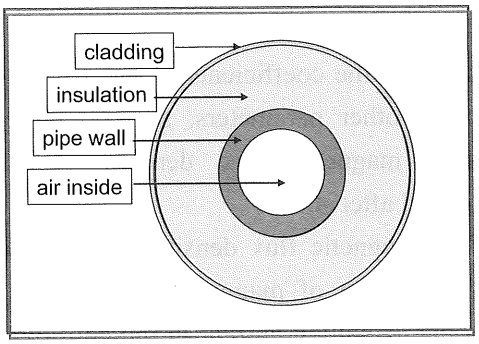

Fig. 1 Top view of a pipe with insulation and cladding.

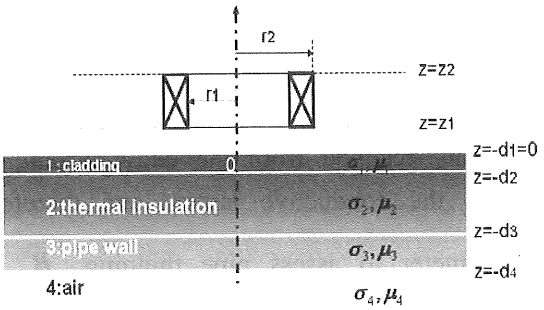

Fig.2 Multi-layered structure.

$$T(t,t+1) = \frac{1}{2}\begin{bmatrix} (1+\frac{\mu_t}{\mu_{t+1}}\frac{\lambda_{t+1}}{\lambda_t})e^{(\lambda_t-\lambda_{t+1})d_{t+1}} & (1-\frac{\mu_t}{\mu_{t+1}}\frac{\lambda_{t+1}}{\lambda_t})e^{(\lambda_t+\lambda_{t+1})d_{t+1}} \\ (1-\frac{\mu_t}{\mu_{t+1}}\frac{\lambda_{t+1}}{\lambda_t})e^{(-\lambda_t-\lambda_{t+1})d_{t+1}} & (1+\frac{\mu_t}{\mu_{t+1}}\frac{\lambda_{t+1}}{\lambda_t})e^{(-\lambda_t+\lambda_{t+1})d_{t+1}} \end{bmatrix} \qquad (4)$$

Consequently, the coefficient C_i and B_i, where i=1,k($k=4$), can be deduced.

$$B_0 = \frac{(\lambda_0\mu_{r1} - \lambda_1)T_{11} + (\lambda_0\mu_{r1} + \lambda_1)T_{21}}{(\lambda_0\mu_{r1} + \lambda_1)T_{11} + (\lambda_0\mu_{r1} - \lambda_1)T_{21}} C_{II} = R(\lambda_0)C_{II} \qquad (5)$$

$$C_k = \frac{2\lambda_0\mu_{r1}}{(\lambda_0\mu_{r1} + \lambda_1)T_{11} + (\lambda_0\mu_{r1} - \lambda_1)T_{21}} C_{II} \qquad (6)$$

and

$$C_t = T(t,k)_{11} C_k, \qquad B_t = T(t,k)_{21} C_k, \qquad (7)$$

where

$T(t,k) = T(t,t+1)T(t+1,t+2)\cdots T(k-1,k)$.

Vector potential A can be calculated by

substituting the coefficients C and B into equation (1). The other parameters, such as eddy current density, magnetic flux density, etc., can be calculated after A.

The magnetic flux density is also regarded as the summation of magnetic flux density resulted from the excitation current in the coil loop and the eddy current in the conductive layers, that is $B = B_s + B_{ec}$. B_s, the magnetic flux density resulted from the excitation current, does not change as far as the excitation coil and excitation current are settled; while B_{ec}, the magnetic flux density resulted from the eddy current, changes with the conductive layers, and therefore is a parameter to assess pipe thinning. B_{ec} can be calculated by the following equation,

$$B_{ec} = \frac{\mu_0 J_c}{2}\int_0^\infty \frac{\Gamma(\lambda_0 r_1, \lambda_0 r_2)}{\lambda_0^2}(e^{-\lambda_0 z_1} - e^{-\lambda_0 z_2})R(\lambda_0)e^{-\lambda_0 z}[J_1(\lambda_0 r)r_0 + J_0(\lambda_0 r)z_0]d\lambda_0 \tag{8}$$

in which

$$R(\lambda_0) = \frac{(\lambda_0\mu_{r1} - \lambda_1)T_{11} + (\lambda_0\mu_{r1} + \lambda_1)T_{21}}{(\lambda_0\mu_{r1} + \lambda_1)T_{11} + (\lambda_0\mu_{r1} - \lambda_1)T_{21}}$$ is

the coefficient reflecting the eddy current effect from the multi conductive layers.

The infinite integration in Eq. (8) can be approximated by

$$B_{ec} = \mu_0 J_c \sum_{i=1}^{\infty} \frac{\Gamma(\lambda_{0i} r_1, \lambda_{0i} r_2)}{\lambda_{0i}[\lambda_{0i}\rho J_0(\lambda_{0i}\rho)]^2}(e^{-\lambda_{0i} z_1} - e^{-\lambda_{0i} z_2})$$
$$R(\lambda_{0i})[J_1(\lambda_{0i} r)r_0 + J_0(\lambda_{0i} r)z_0] \tag{9}$$

By choosing an appropriate number of summation, the magnetic flux density can be calculated with satisfied accuracy.

In case that the multi-layer system is excited by a pulse wave illustrated in Fig. 3, where T is the cycle of pulse, τ the ratio of occupation, the excitation pulse expressed by

$$i(t) = \begin{cases} I_0 & 0 < t < \tau/2 \\ 0 & \tau/2 < t < T/2 \\ -I_0 & T/2 < t < T/2 + \tau/2 \\ 0 & T/2 + \tau/2 < t < T \end{cases} \tag{10}$$

can be approximated by the Fourier series

$$i(t) = \sum_{k=2n+1}^{N} \beta_k [a_k \cos(k\omega t) + b_k \sin(k\omega t)], \tag{11}$$

where N is total number of summation, $\beta_k = \frac{\sin(k\pi/N)}{k\pi/N}$ is the Gibbs factor to reduce the Gibb's phenomenon, and

$$a_k = \frac{2}{k\pi}\sin(k\omega\tau)$$
$$b_k = \frac{2}{k\pi}(1 - \cos(k\omega\tau)) \tag{12}$$

Therefore, the response of magnetic flux density can be calculated by

$$B(t) = \sum_{k=2n+1}^{N} |B_k|\beta_k [a_k \cos(k\omega t + \varphi_k) + b_k \sin(k\omega t + \varphi_k)] \tag{13}$$

where $|B_k|$ and φ_k are respectively the absolute value and the phase angle of the kth order magnetic flux density which can be obtained from Eq. (8).

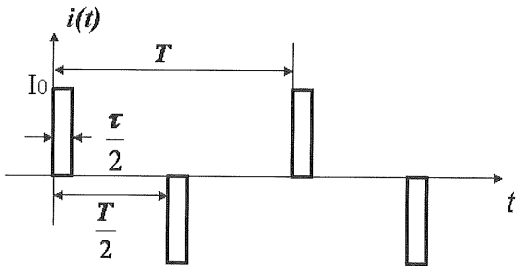

Fig.3 Pulsed excitation current.

2.1 Validation of the Analytical Solution

The analytical solutions are validated by 3D FEM numerical solutions [3].

Figs. 4(a) and (b) show the contours of eddy current density on the cross section of a 10mm thick carbon steel plate, calculated respectively with 3D

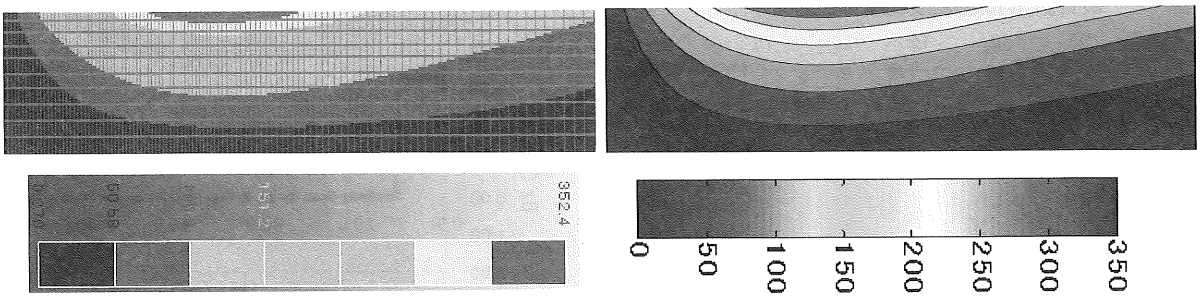

(a) Numerical result (b) Analytical result

Fig. 4 Contour of the eddy current density on the cross section of a 10mm carbon steel plate.

numerical code and the above mentioned analytical solution. The excitation frequency is 10Hz, and excitation current is 30AT. The excitation coil (denoted as EXCOIL-52.5 hereafter), whose inner and outer radius and the thickness are 50mm, 55mm and 10mm, respectively, is held 1mm above the cladding. The cladding (denoted as cladding-M hereafter) whose conductivity and permeability are respectively $1.0\times10^{6}\,\boldsymbol{S/m}$ and 100 is 0.8mm in thickness. The insulation is 29.2mm thick. The conductivity and permeability of the carbon steel (denoted as CBNSTL-A hereafter) are respectively $1.6\times10^{6}\,\boldsymbol{S/m}$ and 1000. Casting aside the difference on color bar, Figs. 4(a) and 4(b) are efficiently identical. This identical on eddy current distribution validates the analytical solution of sinusoidal excitation and implies the applicability of the analytical method in this study.

Fig. 5 shows the magnetic flux density B_z at z=1mm along the axis of a circular coil whose inner and outer radius is respectively 13.25mm and 16.75mm, the coil is 10mm in thickness. The eddy current is initiated by a pulse current whose cycle and occupation rate are 500Hz and 10%, and $\boldsymbol{I}_0$ is 30AT. The B_z signal obtained at the plus half cycle is subtracted by the B_z at the minus half cycle so that common noise is removed. The signal in Fig. 5 is of a half cycle. The signals calculated by the numerical method and the analytical method agree well, excepted at the point of time when excitation current changes dramatically. This may

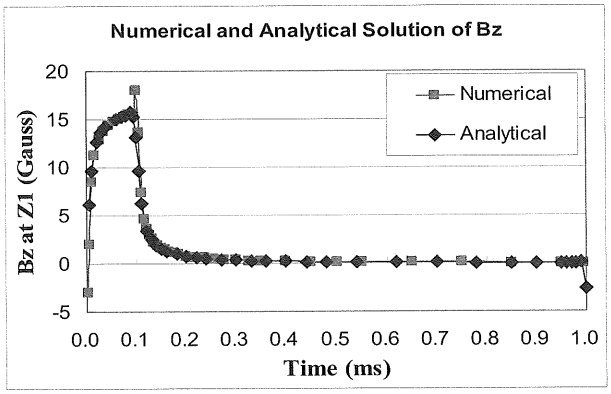

Fig. 5 Pulsed ECT signal of Bz.

be due to the modeling of pulse excitation in numerical calculation. The agreement implies that it is possible to calculate the pulsed eddy current response using analytical solution in Eq. (13).

3. EDDY CURRENT MEASUREMENT OF A FOUR-LAYER STRUCTURE

By applying the analytically approximate solution deduced in last section, we can investigate the capability of eddy current method regarding wall thickness measurement, and see how the signal is affected by inspection conditions.

Parameters reflecting the inspection condition and the multi-layer structure are: the electromagnetic property and thickness of each layer, the excitation current and frequency, and the occupation rate in case of pulse wave, etc.

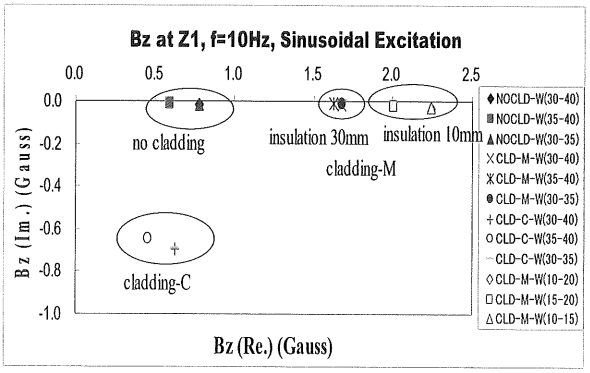

Fig. 6 Simulation of Bz signal obtained from low frequency eddy current measurement.

3.1 Low frequency eddy current method

Magnetic flux densities resulted from the eddy current are calculated along the axis of the circular coil. Fig. 6 shows the normal component of magnetic flux density $\boldsymbol{B}_z^{ec}$ at position Z=1mm, with respect to different cladding layers and insulation/wall thickness. The pipe is made of carbon steel CBNSTL-A. In this figure, NOCLD means without cladding layer, and CLD-M and CLD-C stand for cladding-M and cladding-C, respectively. The XX1 and XX2 in W(XX1-XX2) stand for d_3 and d_4 in Fig. 2. The thickness of the wall is XX1-XX2, and is XX1 below the surface of cladding layer. W(30-40) stands for the normal situation that the wall is 10mm thick and 30mm below the cladding. W(35-40) and W(30-35) represent outer and inner thinning respectively, while the wall is 5mm thick.

No significant difference is observed on Bz signals of W(30-40) and W(30-35). It implies that it is difficult to measure the wall thinning on the inner side of a pipe. However, the difference on the Bz signals of W(30-40) and W(35-40) shows the possibility of measuring the wall thinning on the outer side of a pipe using sinusoidal eddy current method.

The difference between the Bz signals of W(30-40) and W(35-40) with magnetic lagging CLD-M is smaller than that of with non-magnetic lagging CLD-C. Therefore, it is more challengeable

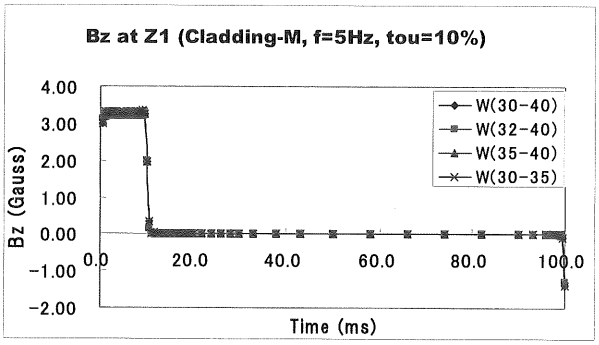

(a) Bz versus time, carbon steel wall of different thickness under magnetic cladding.

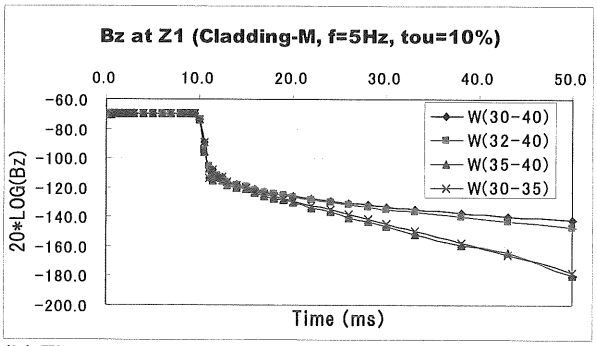

(b) The decaying of Bz of a carbon steel wall under magnetic cladding.

Fig. 7 Magnetic flux density Bz at z=1mm, resulted from carbon steel walls with different thickness, under magnetic cladding.

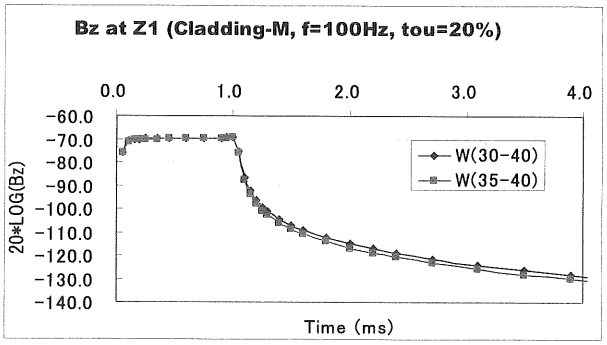

Fig. 8 The decayed Bz versus time. The frequency of excitation pulse is 100Hz.

to measure the thickness of a pipe when the protective cladding layer is magnetic.

Fig. 6 also shows that by reducing the thickness of insulation from 30mm to 10mm, the amplitude of Bz increases. The thicker the insulation layer, the more difficult to measure the wall thickness.

3.2 Pulsed eddy current method

The eddy current is induced by the pulse current described in Fig.3.

Fig. 7(a) show the Bz at Z1 of different thickness CBNSTL-A pipes under 0.8mm cladding-M. The cycle of excitation pulse is 5Hz, and the occupation rate is 10%. The difference on the maximum value of the Bz on Fig.7(a) corresponding to different wall/insulation thickness is very small. However, significant difference is observed on the logarithm value of the decayed Bz. If the measurement equipment is sensitive enough, it is possible to measure the wall thickness using the decayed magnetic flux density signal. The decayed Bz signals of W(30-35) and W(35-40) are almost identical, it implies that the pulsed eddy current method is applicable regardless of inner or outer thinning.

Fig. 8 shows the measurement of the same pipe thinning of Fig. 7 when the cycle of pulse is increased to 100Hz, and the occupation rate is 20%. However, the difference on the decayed signals of the W(30-40) and W(35-40) is much smaller than that at 5Hz. Therefore, it is advisable of using lower frequency pulsed excitation current.

The cladding of Fig. 9 is a non-magnetic conductor whose conductivity is as high as $3.8\times10^{8} S/m$. 2mm wall thinning is detectable from the decayed signal. Comparing Fig. 9 to Fig. 7, we find that the Bz signal of the same pipe under non-magnetic cladding is larger than that of under magnetic cladding-M. Therefore, the wall thinning under magnetic cladding is more difficult to measure.

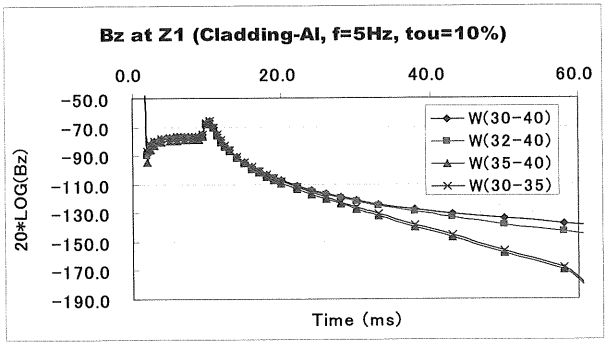

Fig. 9 Decay of Bz, carbon steel pipe under non-magnetic cladding.

4. CONCLUSION

Analytical solution is deduced on a cylindrically symmetric multi-layered conductive/magnetic structure. The solution is validated by 3D numerical solution, and applied to the simulation of wall thinning measurement using both sinusoidal eddy current and pulsed eddy current method. The simulation shows that low frequency sinusoidal eddy current is basically limited for the measurement of outer wall thinning, while pulsed eddy current is valid for both inner and outer wall thinning measurement. It is advisable to use a low cycle pulse for wall thickness measurement. .The electromagnetic property of cladding affects the measurement significantly. Wall thinning under magnetic cladding layers are more difficult to measure than that under non-magnetic ones.

参考文献

[1] C.V.Dodd, W.E.Deeds, "Analytical solutions to eddy-current probe-coil problems", Journal of Applied Physics, Vol. 39, No. 6, 2829-2838 (1968).

[2] C.V.Dodd, C.C.Cheng, and W.E.Deeds, "Indcution coils coaxial with an arbitrary number of cylindrical conductors", Journal of Applied Physics, Vol. 45, No. 2, 638-649 (1974).

[3] w. Cheng, I.Komura, "Simulation of transient eddy-current measurement for the characterization of depth and conductivity of a conductive plate", IEEE Tran. Mag, Vol.44, No. 11, 3281-3284 (2008).